Mechanical Control of Spin States in Spin-1 Molecules and the Underscreened Kondo Effect

J. J. Parks, *et al.*

Science **328**, 1370 (2010);
DOI: 10.1126/science.1186874

Mechanical Control of Spin States in Spin-1 Molecules and the Underscreened Kondo Effect

J. J. Parks,[1,2] A. R. Champagne,[1]* T. A. Costi,[3] W. W. Shum,[2] A. N. Pasupathy,[1]† E. Neuscamman,[2] S. Flores-Torres,[2] P. S. Cornaglia,[4] A. A. Aligia,[4] C. A. Balseiro,[4] G. K.-L. Chan,[2] H. D. Abruña,[2] D. C. Ralph[1,5]‡

The ability to make electrical contact to single molecules creates opportunities to examine fundamental processes governing electron flow on the smallest possible length scales. We report experiments in which we controllably stretched individual cobalt complexes having spin $S = 1$, while simultaneously measuring current flow through the molecule. The molecule's spin states and magnetic anisotropy were manipulated in the absence of a magnetic field by modification of the molecular symmetry. This control enabled quantitative studies of the underscreened Kondo effect, in which conduction electrons only partially compensate the molecular spin. Our findings demonstrate a mechanism of spin control in single-molecule devices and establish that they can serve as model systems for making precision tests of correlated-electron theories.

The electronic states of atoms and molecules depend on the symmetry imposed by their local environment. A simple manifestation occurs in the attachment of ligands to a transition-metal ion to form a coordination complex, which breaks spherical symmetry and causes splittings within the ion's initially degenerate *d* orbitals. For a complex having spin $S \geq 1$, additional distortions of the ligands combined with spin-orbit coupling can cause splittings within the initially $(2S + 1)$-degenerate spin states, giving rise to magnetic anisotropy (*1*, *2*). To study the effects of symmetry-breaking distortions, we stretched individual $S = 1$ molecules within mechanically controllable devices (*3*). Simultaneous electron transport measurements showed that stretching lifts the degeneracy of the $S = 1$ ground state and enables control of the magnetic anisotropy. The same devices also enabled tests of predictions (*4*) for the temperature dependence of the underscreened $S = 1$ Kondo effect (*5*–*7*).

We studied the $Co(tpy\text{-}SH)_2$ complex (where tpy-SH is 4′-mercapto-2,2′:6′,2″-terpyridine) (Fig. 1A), in which a Co ion resides in an environment of approximate octahedral symmetry, through its coordination to six N atoms on two terpyridine ligands. When attached to gold electrodes and cooled to low temperature, this molecule exhibits the Kondo effect (*8*); the spin of the molecule is screened by electron spins in the electrodes, leading to a peak in the electrical conductance at zero bias voltage, V (*9*). We used the Kondo effect as a spectroscopic probe to interrogate the molecular spin (*10*). Previous electron-transport studies of individual metal complexes have probed rich behavior, including not only Kondo physics (*8*, *11*–*13*) but also vibrational excitations (*13*–*15*) and molecular magnetism (*16*, *17*).

We used mechanically controllable break-junction devices (Fig. 1B) to stretch individual molecules while measuring their conductance. The devices were made by fabricating a Au wire suspended above a thin Si substrate (Fig. 1C), depositing molecules, and then using electromigration (*18*) to create a molecular-scale break in the wires before beginning studies in which we tuned the distance between electrodes by bending the substrate. Details, statistics, and discussion of control experiments are provided in (*19*). We have also measured the same $Co(tpy\text{-}SH)_2$ complex by using fixed Au electrodes (*8*, *11*, *13*, *15*–*17*).

Measurements of differential conductance (dI/dV) as a function of increasing electrode spacing at a temperature $T = 1.6$ K are shown in Fig. 2. At the initial position of the electrodes, the dI/dV spectra exhibited a single peak centered at $V = 0$ with amplitude of order (but less than) $2e^2/h$, a signature of Kondo-assisted tunneling through the molecule. As we stretched each molecule, the single conductance peak split into two beyond a value for the change in electrode spacing that varied from device to device. For the two devices displayed in Fig. 2 and for two others [supporting online material (SOM) section S2], we could reproducibly cross this transition back and forth between one peak and two. For the stretched molecules (Fig. 2E), the temperature dependence of dI/dV at $V = 0$ showed a nonmonotonic dependence similar to the V dependence upon increasing $|V|$ from 0.

The observed splitting of the Kondo peak as a function of stretching is in contrast to a previous study of the spin-½ Kondo effect in C_{60} molecules (*20*), in which varying the electrode spacing modified the height and width of the Kondo resonance but did not split the peak. We show that the peak splitting for the $Co(tpy\text{-}SH)_2$ complex is caused by a higher-spin $S = 1$ Kondo effect, together with the breaking of degeneracy within the $S = 1$ triplet ground state caused by molecular distortion (*2*). For an unstretched $S = 1$ ion in a ligand field with octahedral symmetry, the triplet states are strictly degenerate according to group theory. However, if the molecule is stretched axially (the z axis), the $S_z = 0$ state will be lowered by a zero-field splitting energy D be-

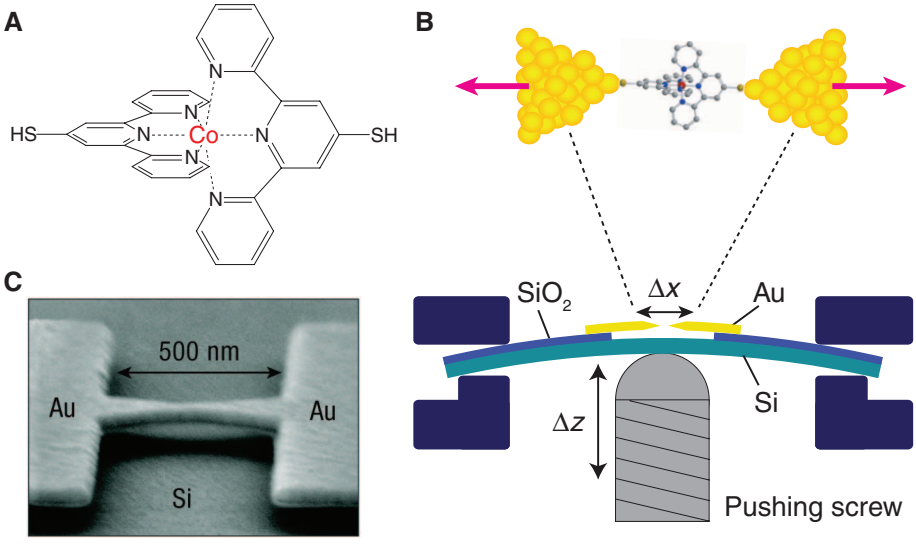

Fig. 1. Single-molecule electrical devices based on a transition-metal complex. (**A**) Chemical structure of $Co(tpy\text{-}SH)_2$, where tpy-SH is 4′-mercapto-2,2′:6′,2″-terpyridine. (**B**) Schematic of the mechanically controllable break junction. (**C**) Scanning electron micrograph of a suspended break junction before molecule deposition.

[1]Laboratory of Atomic and Solid State Physics, Cornell University, Ithaca, NY 14853, USA. [2]Department of Chemistry and Chemical Biology, Cornell University, Ithaca, NY 14853, USA. [3]Institut für Festkörperforschung and Institute for Advanced Simulation, Forschungszentrum Jülich, 52425 Jülich, Germany. [4]Centro Atómico Bariloche and Instituto Balseiro, Comisión Nacional de Energía Atómica (CNEA), Consejo Nacional de Investigaciones Científicas y Técnicas (CONICET), 8400 San Carlos de Bariloche, Argentina. [5]Kavli Institute at Cornell, Cornell University, Ithaca, NY 14853, USA.

*Present address: Department of Physics, Concordia University, Montréal, Québec H4B 1R6, Canada.

†Present address: Department of Physics, Columbia University, New York, NY 10027, USA.

‡To whom correspondence should be addressed. E-mail: ralph@ccmr.cornell.edu

low the $S_z = \pm 1$ states, corresponding to a uniaxial spin anisotropy (Fig. 2F). This broken degeneracy quenches the Kondo resonance near $V = 0$ and causes conductance peaks at $V = \pm D/e$ because of inelastic tunneling. The distortion-induced breaking of the ground-state degeneracy for an $S = 1$ molecule is in contrast to the physics of half-integer spins (*21*) for which time-reversal symmetry mandates that the ground state remains a degenerate Kramers doublet. To establish this picture of stretching-induced control of spin states, we show that the spin of our molecules is indeed $S = 1$, on the basis of temperature and magnetic-field studies, and we verify that stretching produces spin anisotropy by measuring how the level splitting depends on the direction of an applied magnetic field.

The temperature dependence of the Kondo conductance is predicted to depend on the molecular spin, S, and the number of screening channels in the electrodes. To be fully screened at zero temperature, a molecule with spin S requires coupling to $2S$ screening channels (*5*). In our experimental geometry, there are two screening channels consisting of linear combinations of states from the two electrodes with different couplings J_1 and J_2 to the molecular spin that result in two Kondo temperature scales, T_{K1} and T_{K2} (*22*) (we assume $T_{K1} < T_{K2}$). The Kondo temperatures depend exponentially on the couplings, so in the typical case T_{K1} is much smaller than T_{K2}. If $S > 1/2$, the result is that over the range $T_{K1} << T < T_{K2}$ the original spin is only partially screened, to a value $S - 1/2$. Relative to the fully screened $S = 1/2$ Kondo effect, this underscreened effect should produce a much slower rise in the conductance as T decreases below T_{K2} (*4*, *6*, *7*). Henceforth we denote T_{K2} as simply T_K.

Figure 3, A and B, shows the measured zero-bias conductance $G(T)$ for the unstretched configuration of devices A and B with fits to numerical renormalization group (NRG) predictions for the fully screened $S = 1/2$ Kondo model (*23*, *24*) and the underscreened $S = 1$ and 3/2 models (*4*) (for fitting details, see SOM S3). Each fit has two adjustable parameters, T_K and the zero-temperature conductance $G(0)$. We find that $G(T)$ deviates strongly from the form for the $S = 1/2$ Kondo effect and instead agrees quantitatively with the prediction for the $S = 1$ underscreened case. We performed the same analysis for 10 unstretched

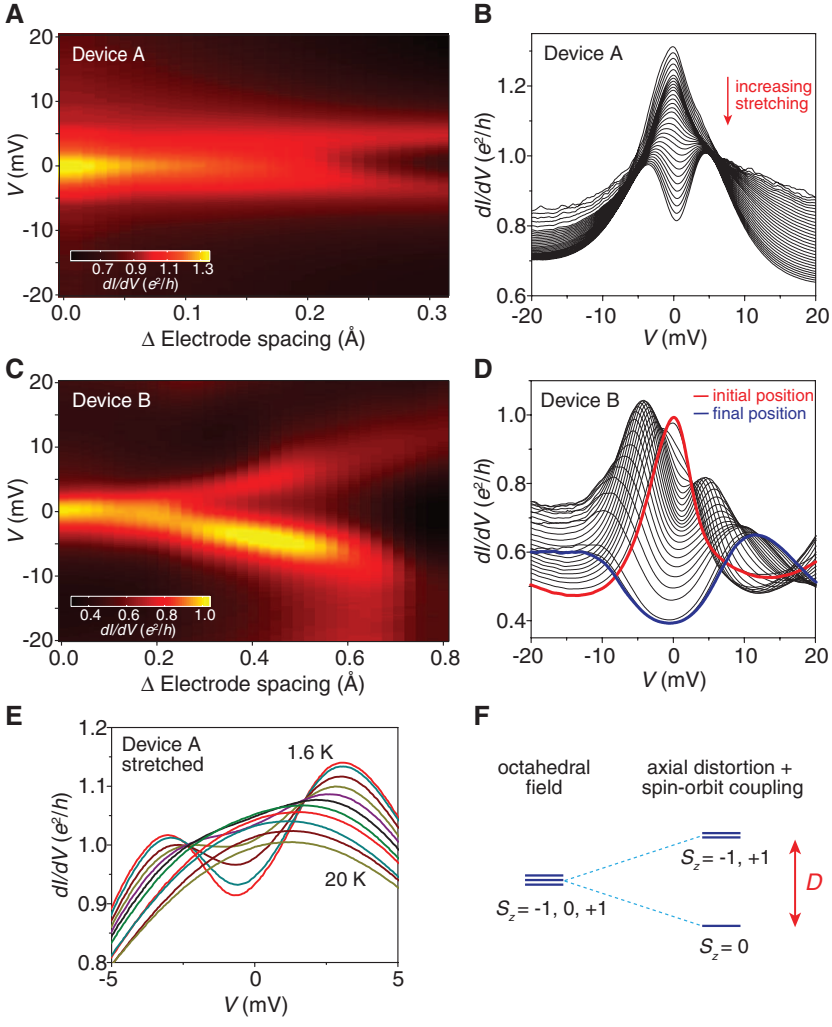

Fig. 2. Splitting of the Kondo peaks as a function of mechanical stretching. (**A** and **C**) *dI/dV* as a function of bias voltage and electrode spacing at $T = 1.6$ K for (A) device A and (C) device B. (**B** and **D**) Line cuts showing *dI/dV* as a function of V for different values of molecular stretching for (B) device A and (D) device B. (**E**) Temperature dependence of the conductance for device A on the stretched side of the splitting transition. (**F**) Breaking of the degeneracy among the $S = 1$ triplet states by uniaxial distortion.

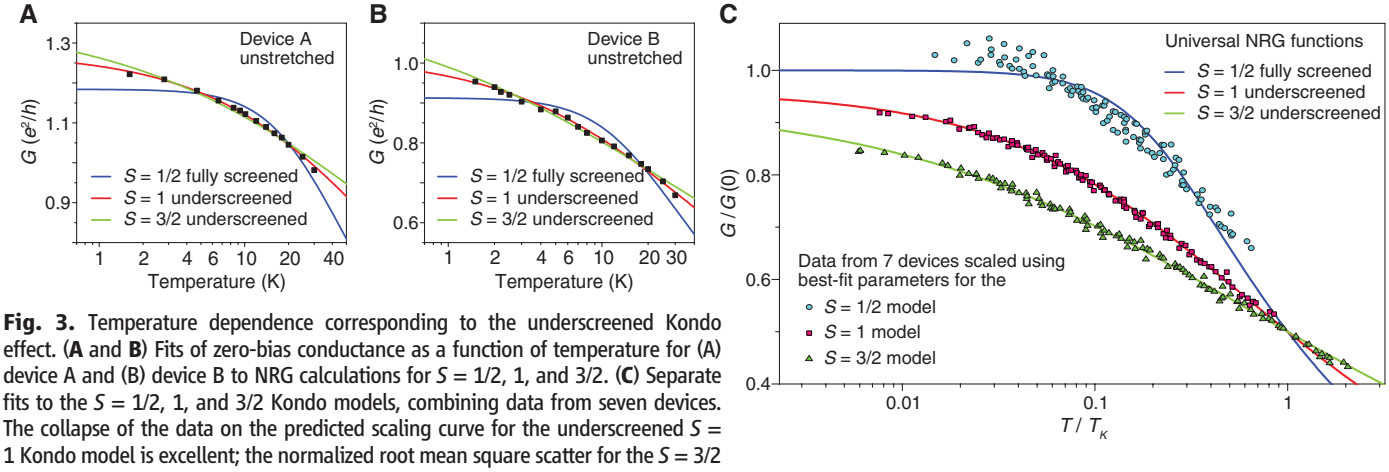

Fig. 3. Temperature dependence corresponding to the underscreened Kondo effect. (**A** and **B**) Fits of zero-bias conductance as a function of temperature for (A) device A and (B) device B to NRG calculations for $S = 1/2$, 1, and 3/2. (**C**) Separate fits to the $S = 1/2$, 1, and 3/2 Kondo models, combining data from seven devices. The collapse of the data on the predicted scaling curve for the underscreened $S = 1$ Kondo model is excellent; the normalized root mean square scatter for the $S = 3/2$ ansatz is greater by 44% and for $S = 1/2$ by 320%. For the $S = 1$ fits, the seven Kondo temperatures are 1.1, 28, 62, 81, 84, 180, and 210 K.

$Co(tpy\text{-}SH)_2$ devices (SOM S4). Seven showed similarly unambiguous agreement with underscreened Kondo scaling, and all of these gave superior fits to the $S = 1$ prediction than to $S = 3/2$. Discussion of the other three samples is provided in SOM S4.

In Fig. 3C, for the seven devices with underscreened characteristics, we plotted $G(T)/G(0)$ versus T/T_K by using the parameters $G(0)$ and T_K obtained from separate fits to the $S = 1/2$, 1, and 3/2 models. This allowed us to test how well the data can all be described by the predicted scaling curves. We used the root mean square deviation of the data from each theory curve normalized to the average of the scaled data as a goodness-of-fit metric. The $S = 1$ fit is best: The deviation of points for the $S = 1/2$ ansatz is greater by 320%, for $S = 3/2$ by 44%, and for larger S by more than 80%. Additional confirmation that $S = 1$ is discussed below based on magnetic field studies. An independent (*25*) observation of the temperature scaling predicted for the underscreened Kondo effect has also been reported recently for a single $S = 1$ C_{60} device (*26*).

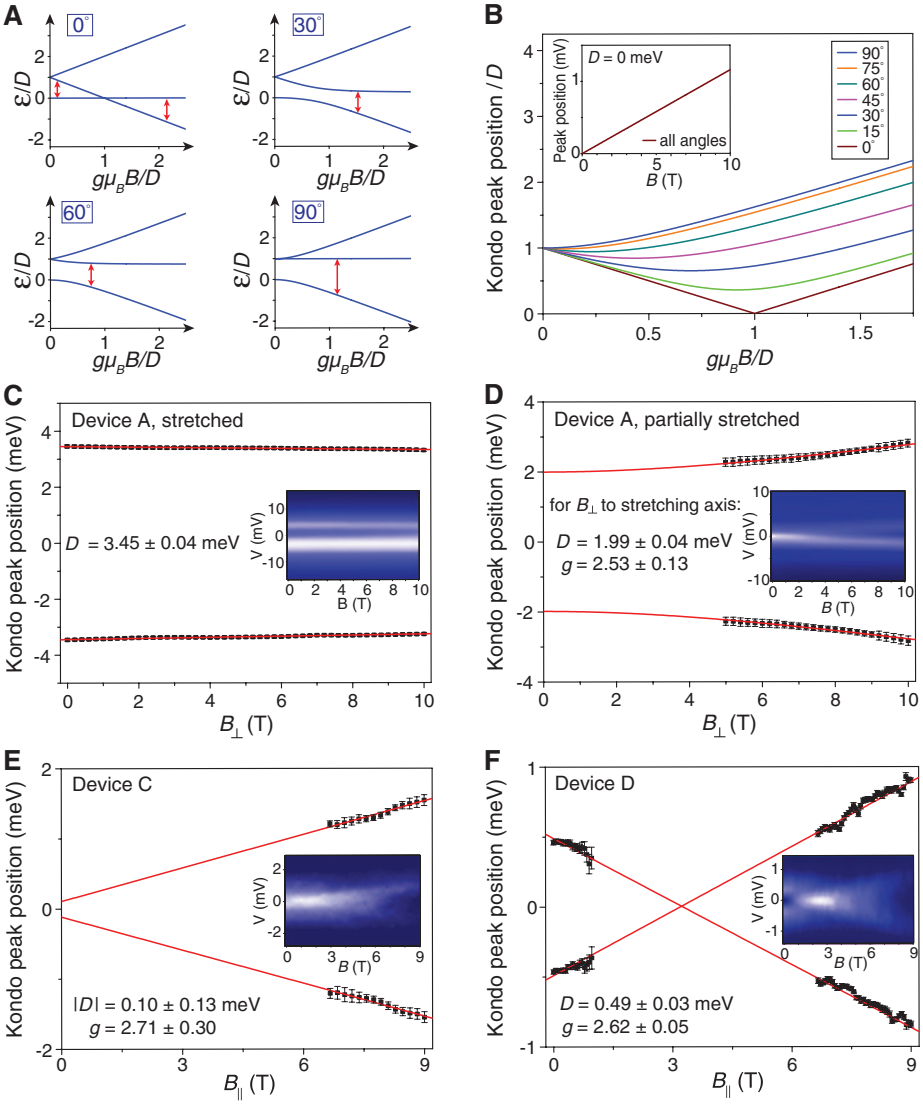

Fig. 4. The magnetic field evolution of the Kondo peaks demonstrates the presence of spin anisotropy. (**A**) Energy eigenvalues (for $S = 1$) of the model spin-anisotropy Hamiltonian $H = -g\mu_B \boldsymbol{B}\cdot\boldsymbol{S} + DS_z^2$ for four different field angles with respect to the anisotropy axis. The red arrows indicate the lowest-energy inelastic transitions corresponding to the finite-bias Kondo peaks. (**B**) Predicted Kondo peak position versus magnetic field at several field angles, with energies normalized to the zero-field splitting. (Inset) Kondo peak splitting (for $g = 2$) as a function of magnetic field for all angles in the absence of spin anisotropy. (**C** and **D**) Kondo peak positions versus magnetic field at $T = 1.6$ K in device A for two different values of stretching with the magnetic field oriented approximately perpendicular to the molecule axis. The data in (D) can be fit for any field angle between 70° and 90°, giving parameters in the range $D = 2.0$ to 2.2 meV and $g = 2.5$ to 2.8. (**E** and **F**) The magnetic field dependence in fixed-electrode devices C and D with the magnetic field approximately along the molecular axis. (Insets) Color plots of *dI/dV* versus bias voltage and magnetic field.

Our interpretation that the stretching-induced Kondo splitting is caused by the breaking of spin degeneracy is confirmed by the presence of spin anisotropy in the stretched state: the magnetic field (B) dependence of the Kondo splitting differs depending on the angle at which B is applied relative to the stretching axis. Figure 4A shows the expected B dependences of the energy levels in an $S = 1$ multiplet for $D > 0$ and for several field angles, and Fig. 4B displays the energy differences between the first excited state and the ground state, which determine the Kondo peak positions. For a field orientation approximately perpendicular to the anisotropy axis ($\theta = 90°$), when $g\mu_B B \ll D$ (where μ_B is the Bohr magneton) the B dependence of the peak position should be very weak, whereas when $g\mu_B B$ grows large enough to be comparable to D, the peak should shift gradually to larger values of $|V|$ with positive curvature. For B parallel to the anisotropy axis ($\theta = 0°$), the B dependence of the peak position should be linear and much stronger. Our measurements show a dependence on the orientation of B just as expected within this model. Figure 4, C and D, shows the B dependence for different degrees of stretching for device A, with $\theta \approx 90°$. At a relatively large degree of stretching (Fig. 4C), $D = 3.45$ meV was larger than $g\mu_B B$ at our largest field (~1.5 meV), and the Kondo peak positions were almost independent of B. The slightly negative slope of $d|V|/dB$ [corresponding to an effective g factor of 0.21 ± 0.01 (SD)] suggests that the stretching axis is not exactly perpendicular to B. For a smaller degree of stretching (Fig. 4D), $g\mu_B B$ was comparable to D at large fields, and the Kondo peaks shifted weakly to larger $|V|$ as a function of B with positive curvature. Figure 4, E and F, shows data for B approximately parallel to the molecular axis for fixed-electrode devices, which exhibit zero-field splitting without intentional mechanical stretching (among devices that had Kondo features, ~10% of the fixed-electrode devices and ~20% of the adjustable devices exhibited a split Kondo peak at the initial electrode spacing, suggesting that these molecules happened to be strained initially). In Fig. 4, E and F, the Kondo peaks shift linearly with B, with much larger slopes of $d|V|/dB$ than for $\theta \approx 90°$, corresponding to g factors of 2.6 to 2.7 (± 0.3). In device D, the peaks shift initially to smaller $|V|$, pass through zero, and then move to larger $|V|$ (Fig. 4F). From the negative slopes of $d|V|/dB$ in Fig. 4, C and F, we can confirm that $D > 0$. The scale of splittings we measure, ~0 to 5 meV, agrees with our simulations (SOM S6) and is typical of zero-field splittings in distorted coordination complexes (*2*).

These magnetic field data provide further evidence that the spin state of the molecule is $S = 1$, rather than 1/2, 3/2, or any half integer. For half-integer spins with $D > 0$, the ground state for $B = 0$ is the degenerate Kramers doublet $S_z = \pm 1/2$. Regardless of the direction of B or the degree of stretching, this doublet will give rise to a Kondo peak that shifts approximately linearly with B and

extrapolates to zero splitting at $B = 0$ (*21*), in contradiction to the data (SOM S7). Integer values of $S \geq 2$ can be ruled out on the basis of the temperature scaling described above and because previous studies of sixfold coordinated Co complexes have found almost exclusively $S \leq 3/2$, with exceptions only for fluoride ligands (*1*, *2*). We conclude that only $S = 1$ can explain the measurements, and from this we identify the charge state of the metal center to be Co^{1+} (SOM S8).

In coordination chemistry, the existence of zero-field splittings induced by molecular distortion is well established, but the ability we demonstrate to continuously distort an individual molecule while simultaneously measuring its zero-field splitting opens the possibility for dramatically more detailed and precise comparisons with theory. For correlated-electron physics, our results demonstrate that single-molecule electrical devices can provide well-controlled model systems for studying $S \geq 1$ underscreened Kondo effects not previously realizable in experiment. Our work further demonstrates that mechanical control can be a realistic strategy for manipulating molecular spin states to supplement or replace the use of magnetic fields in proposed applications such as quantum manipulation or information storage (*27*, *28*).

References and Notes

1. A. Abragam, B. Bleaney, *Electron Paramagnetic Resonance of Transition Ions* (Dover, New York, 1986).
2. R. Boca, *Coord. Chem. Rev.* **248**, 757 (2004).
3. N. Agraït, A. L. Yeyati, J. M. van Ruitenbeek, *Phys. Rep.* **377**, 81 (2003).
4. F. Mallet *et al.*, *Phys. Rev. Lett.* **97**, 226804 (2006).
5. P. Nozières, A. Blandin, *J. Phys. (Paris)* **41**, 193 (1980).
6. A. Posazhennikova, P. Coleman, *Phys. Rev. Lett.* **94**, 036802 (2005).
7. P. Mehta, N. Andrei, P. Coleman, L. Borda, G. Zarand, *Phys. Rev. B* **72**, 014430 (2005).
8. J. Park *et al.*, *Nature* **417**, 722 (2002).
9. M. Grobis, I. G. Rau, R. M. Potok, D. Goldhaber-Gordon, in *Handbook of Magnetism and Advanced Magnetic Materials*, H. Kronmüller, S. S. P. Parkin, Eds. (Wiley, Hoboken, NJ, 2007).
10. C. Romeike, M. R. Wegewijs, W. Hofstetter, H. Schoeller, *Phys. Rev. Lett.* **97**, 206601 (2006).
11. W. Liang, M. P. Shores, M. Bockrath, J. R. Long, H. Park, *Nature* **417**, 725 (2002).
12. A. Zhao *et al.*, *Science* **309**, 1542 (2005).
13. L. H. Yu *et al.*, *Phys. Rev. Lett.* **93**, 266802 (2004).
14. X. H. Qiu, G. V. Nazin, W. Ho, *Phys. Rev. Lett.* **92**, 206102 (2004).
15. D.-H. Chae *et al.*, *Nano Lett.* **6**, 165 (2006).
16. H. B. Heersche *et al.*, *Phys. Rev. Lett.* **96**, 206801 (2006).
17. M.-H. Jo *et al.*, *Nano Lett.* **6**, 2014 (2006).
18. H. Park, A. K. L. Lim, A. P. Alivisatos, J. Park, P. L. McEuen, *Appl. Phys. Lett.* **75**, 301 (1999).
19. Materials and methods are available as supporting material on *Science* Online.
20. J. J. Parks *et al.*, *Phys. Rev. Lett.* **99**, 026601 (2007).
21. A. F. Otte *et al.*, *Nat. Phys.* **4**, 847 (2008).
22. M. Pustilnik, L. I. Glazman, *Phys. Rev. Lett.* **87**, 216601 (2001).
23. T. A. Costi, A. C. Hewson, V. Zlatic, *J. Phys. Cond. Matter* **6**, 2519 (1994).
24. D. Goldhaber-Gordon *et al.*, *Phys. Rev. Lett.* **81**, 5225 (1998).
25. J. J. Parks, thesis, Cornell University, Ithaca, NY (2009).
26. N. Roch, S. Florens, T. A. Costi, W. Wernsdorfer, F. Balestro, *Phys. Rev. Lett.* **103**, 197202 (2009).
27. G. Christou, D. Gatteschi, D. N. Hendrickson, R. Sessoli, *MRS Bull.* **25**, 66 (November 2000).
28. L. Bogani, W. Wernsdorfer, *Nat. Mater.* **7**, 179 (2008).

29. We thank I. Cohen, M. Grobis, G. Hutchison, and P. McEuen for discussions and K. Bolotin, J. Grose, F. Kuemmeth, and E. Tam for technical help. Research at Cornell was supported by the NSF through the Cornell Center for Materials Research, DMR-0605742, CHE-0403806, and use of the Cornell Nanofabrication Facility/National Nanotechnology Infrastructure Network. T.A.C. acknowledges supercomputer support by the John von Neumann Institute for Computing (Jülich). P.S.C., A.A.A., and C.A.B. were supported by Proyectos de Investigación Plurianuales 11220080101821 of CONICET.

Supporting Online Material

www.sciencemag.org/cgi/content/full/328/5984/1370/DC1
Materials and Methods
SOM Text
Figs. S1 to S8
Table S1
References

11 January 2010; accepted 29 April 2010
10.1126/science.1186874

Nanoscale Tunable Reduction of Graphene Oxide for Graphene Electronics

Zhongqing Wei,[1*] Debin Wang,[2*] Suenne Kim,[2] Soo-Young Kim,[3,4] Yike Hu,[2] Michael K. Yakes,[1] Arnaldo R. Laracuente,[1] Zhenting Dai,[5] Seth R. Marder,[3] Claire Berger,[2,6] William P. King,[5] Walter A. de Heer,[2] Paul E. Sheehan,[1]† Elisa Riedo[2]†

The reduced form of graphene oxide (GO) is an attractive alternative to graphene for producing large-scale flexible conductors and for creating devices that require an electronic gap. We report on a means to tune the topographical and electrical properties of reduced GO (rGO) with nanoscopic resolution by local thermal reduction of GO with a heated atomic force microscope tip. The rGO regions are up to four orders of magnitude more conductive than pristine GO. No sign of tip wear or sample tearing was observed. Variably conductive nanoribbons with dimensions down to 12 nanometers could be produced in oxidized epitaxial graphene films in a single step that is clean, rapid, and reliable.

Graphene's high electronic mobility (*1*) has been harnessed in devices such as transistors operating at gigahertz frequency (*2*); however, the zero band gap of graphene leads to high leakage currents in many applications. Another interesting material for a range of applications is graphene oxide (GO) (*3*, *4*), which exhibits a transport gap greater than 0.5 eV at room temperature and becomes a semiconductor or semimetal as it is reduced back toward graphene (*5*, *6*). Reduced GO (rGO) resembles graphene but with some residual oxygen and structural defects, yielding a conductivity that is comparable to that of doped conductive polymers (*7*) and 33,000 times higher than that of doped hydrogenated amorphous Si (*8*). Reduced GO can also be used in highly sensitive gas sensors (*9*) and mechanical resonators with figures of merit surpassing those of graphene resonators (*10*).

We present a tip-based thermochemical nanolithography method to control the extent of reduction of GO and pattern nanoscale regions of rGO within a GO sheet at speeds of several μm/s. The relative increase in conductivity is as high as four orders of magnitude. GO was converted to rGO with a 100% yield in dozens of structures patterned on random locations in the GO film. Reduced GO patterns range from ribbons 12 nm in width (full width at half maximum, FWHM) up to 20 μm. No sign of tip wear or sample tearing was observed, indicating that the "carbon skeleton" is continuous across the GO/rGO junction. Thermochemical nanolithography (TCNL) with heated probe tips can localize thermally induced chemical reactions on a surface (*11*–*14*) or deposit material (*15*–*17*). Similar heated tips have also been used to mechanically modify a polymer film (*18*). We performed TCNL by using a heated atomic force microscope (AFM) probe tip to reduce selected regions of both single layers of isolated GO and large-area GO films formed by on-chip oxidation of epitaxial graphene (GO_{epi}) grown on SiC.

Exposure of GO to strong reducing agents like hydrazine results in an increased electrical conductivity by three to four orders of magnitude (*19*). Thermal reduction of GO occurs already at moderate temperature (100° to 250°C) and enables tuning the gap in graphene oxide (*6*), as demonstrated in its current-voltage (*I*-*V*) characteristics. Recent studies have shown that annealing

[1]Chemistry Division, U.S. Naval Research Laboratory, Code 6177, Washington, DC 20375, USA. [2]School of Physics, Georgia Institute of Technology, Atlanta, GA 30332, USA. [3]School of Chemistry and Biochemistry, Georgia Institute of Technology, Atlanta, GA 30332, USA. [4]School of Chemical Engineering and Materials Science, Chung Ang University, Seoul 156-756, Republic of Korea. [5]Department of Mechanical Science and Engineering, University of Illinois Urbana-Champaign, Urbana, IL 61801, USA. [6]CNRS-Institut Néel, BP166, 38042 Grenoble Cedex 9, France.

*These authors contributed equally to this work.
†To whom correspondence should be addressed. E-mail: paul.sheehan@nrl.navy.mil (P.E.S.); elisa.riedo@physics.gatech.edu (E.R.)